Bull. Pharm. Sci., Assiut University, Vol. 47, Issue 2, 2024, pp. 989-1008.

Bulletin of Pharmaceutical Sciences
Assiut University
Website: http://bpsa.journals.ekb.eg/

BULL. PHARM. SCI. Assiut Univ.

COMPUTATIONAL SELECTION AND OPTIMIZATION OF RNA APTAMER AGAINST ALPHA-FETOPROTEIN- AN *IN SILICO* STUDY

Muhamad Muhamad Alkriz*, Dima Joujeh

Department of Biotechnology engineering, Faculty of Technical engineering, University of Aleppo, Syria

Liver cancer ranks the fourth leading cause of cancer-related deaths worldwide, with more than 8.4 million new cases. Hepatocellular carcinoma (HCC) is the most common type of liver cancers. In this study, the computational approach was used to develop an RNA aptamer against the AFP protein, which is the most commonly used biomarker for HCC. Random RNA sequences were used as a source for the study, and several rounds of mutations have been introduced to these sequences in order to enhance binding affinity. Molecular docking, and molecular dynamics were utilized to screen aptamers and characterize the detailed interactions between the selected aptamer and the protein. As a result, the selected aptamer (5'-GGAUCGGUGGCCAAGUUAGUCAAACCCCGUGUGCCGGUUUAGCAUAGCCCCGAUCC -3') showed good binding affinity to the target AFP. The RMSF, hydrogen bonds,and RMSD analysis showed that the aptamer-protein complex had lower flexibility, stable, and compact during the time of the simulation. Thus, it can serve as a good candidate for the diagnosis or treatment of liver cancer.

Keywords: *Aptamer; In Silico; AFP; Molecular Dynamics; Molecular Docking*

INTRODUCTION

Liver cancer is the fourth leading cause of cancer-related death worldwide, with approximately 7.8 million deaths annually[1] . Hepatocellular carcinoma (HCC) is the most common type of liver cancer[2] . Alpha-fetoprotein (AFP) is the most commonly used biomarker for HCC[1] .

It is a multi-functional glycoprotein, and belongs to an albumin protein family. It contains (591) amino acids, encoded by a gene located on chromosome 4[3] . This protein is a single polypeptide chain of 70-kDa containing 3% to 5% carbohydrates. It shows a triplicate domain structure formed by intramolecular loops dictated by disulfide bridging[4] , and exhibits a V-shaped form[5] . Inhibition of AFP function may be an effective approach to HCC-specific anticancer treatment[6] . Among various biomolecular recognition elements (antibodies, enzymes, etc.), aptamers are ideal tools for biomedical molecular recognition[7] . Aptamers are short and single-stranded RNA or DNA molecules, approximately 20–100 bases long[8] . They can bind specifically to their targets and induce biochemical effects (e.g., activation, inhibition, denaturation, etc.)[9] . Aptamers can be obtained from random oligonucleotide libraries using systematic evolution of ligands by exponential enrichment (SELEX) technology (SELEX). However, this technology consists of multiple rounds of selection, and is time-consuming, and expensive[10] .

Additionally, aptamers selected using this method need to be truncated to obtain smaller aptamers[11] . Therefore, much research has been performed to develop new methods to produce aptamers with high efficiency, performance, resource-saving, and a greater potential for success[12]. Alternative strategies to SELEX that have been proposed over the past 15 years apply computational bioinformatics methods, namely docking and molecular dynamics[13], to facilitate the design of aptamers and investigate

Received : 26/6/2024 & Accepted : 22/8/2024

*Corresponding author: Muhamad Muhamad Alkriz, E-mail: muhamadalkriz@gmail.com

their binding affinities to their targets[14]. This study aimed to select RNA aptamers targeting AFP in silico. Random RNA sequences were used as a source for the study. We predicted the secondary structure of RNA from its nucleotide sequence, and created a three-dimensional model (tertiary structure). Later, the 3D model was used in molecular docking to determine the binding affinity of the selected aptamer against AFP, and investigate poses of the RNA-protein interaction. Finally, molecular dynamics (MD) simulation was performed to determine the binding stability of the complex.

MATERIALS AND METHODS

Structure Retrieval

The cryo-electron microscopy (cryo-EM) structure of human AFP with a resolution of 2.60 Å was retrieved from the RCSB Protein Data Bank (PDB) (PDB ID: 7YIM). .

Virtual screening to select RNA aptamers

One hundred random RNA sequences of a given length (40- 55 nucleotides), and CG content (> 40%), were generated using the Random Sequence Generator tool provided by Molbiotools (https://molbiotools.com/).

The primary RNA sequences were further examined using the RNAfold server (http://rna.tbi.univie.ac.at/cgi-bin/RNAWebSuite/RNAfold.cgi) for secondary structures prediction, using the following options: minimum free energy (MFE) only, and avoid isolated base pairs (Fold algorithms and basic options); RNA parameters, rescale energy parameters to given temperature (37°C), and a salt concentration of 1.021 molar (Energy parameters). The RNAfold computes the MFE and prints the MFE structure in bracket notation. The RNA sequences and the dot-bracket secondary structure notations were input into the RNA Composer server (https://rnacomposer.cs.put.poznan.pl/)[15, 16] to build the 3D model.

The 3D structures of the random sequences were docked with the protein (AFP) to identify the best-bound aptamer. The docking was performed using the HDOCK server (http://hdock.phys.hust.edu.cn/), and no binding site was identified[17-22]. The top five aptamers with the highest affinity to the target were determined based on the best docking scores.

Aptamer optimization and molecular docking

The aptamer sequence with the the best docking score was selected, and random mutations were introduced in its sequence to produce new sequences, in order to enhance binding affinity and get a more stable structure. The last five nucleotides at both the 5' and 3' ends of the sequence were also designed to be complementary with each other. ENDMEMO's tool (https://www.endmemo.com/bio/gc.php) was used to determine the CG content and the length of the sequences specifically. Subsequently, the generated sequences were docked with the target (AFP), and the mutated sequence with the best score was selected for additional rounds of mutation to achieve good binding affinity and low free energy. Three mutant sequences were generated and docked to the AFP using different docking platforms (HDOCK, MdockPP, and NPdock).

HDOCK

The tertiary structures derived from RNAComposer served as ligand inputs, while the AFP functioned as the receptor. This was executed without the specification of a template or binding site. Several docking models were generated, with emphasis placed on selecting the models exhibiting the best docking scores for each aptamer. The top ten scoring structures for each aptamer were subsequently employed for calculating the Zh-score.

Mdockpp

The initiation point was the "Start from Structure" option. Job type parameters were set as "Heterodimeric," encompassing both Receptor and Ligand, mirroring the approach adopted with HDOCK. The "Straight to job submission" option was selected, while other parameters were maintained at default settings. The top ten scoring structures for each aptamer were subsequently employed for calculating the Zm-score.

NPdock

In the NPdock server, the RNA-protein configuration was chosen. The AFP was loaded

into the protein box, and the aptamer was placed in the RNA/DNA box. No specific Interfaces filtering was employed in this step. The top ten scoring structures for each aptamer were subsequently employed for calculating the Zn-score, and the binding model with the best score was downloaded for subsequent interaction analysis.

Z-score

The obtained docking scores from the docking platforms (HDOCK, MdockPP, and NPdock) were normalized using the following equation: $Z = (I - \bar{I}) / SD$[23]

I: is the docking score of each RNA-protein complex (in a set of top ten binding models). $\bar{I}$: is the average of the docking scores. SD: is the standard deviation. The most negative Z-score in a set of top ten binding models of an aptamer-AFP complex was identified as the Z-score of the complex. The total Z-score (ZT) was calculated by adding the Z-scores of HDOCK (Zh), Mdockpp (Zm), and Npdock (Zn).

Interaction Profiling

The interaction of the three mutant RNA sequences with the protein (AFP) was analyzed in detail to report the nucleotides and amino acids involved in the interactions, using the Protein-Ligand Interaction Profiler (PLIP) server (https://plip-tool.biotec.tu-dresden.de/plip-web/plip/index)[24]. This analysis provides valuable insights into the molecular interactions occurring at the binding interface, such as hydrogen bonds (H-bonds), π-stacking, hydrophobic interactions, and ionic interactions.

Molecular dynamics (MD) simulation

The work was taken forward to better study the dynamics of the aptamer-protein complex. MD simulation was performed based on the best configuration of the aptamer- AFP complex obtained from docking, to predict the atomic mobility of the simulated system over time. The CHARMM36m force field was used for the simulation of the system. The initial complex configuration was generated using the Charmm-gui Solution Builder feature (https://www.charmm-gui.org)[25, 26, 27] based on the provided PDB files. The simulation was performed using NAMD v3.0b4 (https://www.ks.uiuc.edu/Research/namd)[28]. The simulation system was prepared in a rectangular periodic cubic box, hydrated with a TIP3P water model, and neutralized by adding 0.15 M NaCl ions. The total time of MD simulation was 32.58 nanoseconds under periodic boundary conditions. The resulting trajectory data from the simulation was analyzed using VMD v 1.9.4a53[29]. Key parameters such as root-mean-square deviation (RMSD), radius of gyration (Rg), root-mean-square fluctuation (RMSF), and hydrogen bond interactions (H-bonds) were calculated.

Graphical Images

All representations of pictorial structures were generated utilizing VMD-Visual Molecular Dynamics v1.9.4a53 (Theoretical and Computational Biophysics Group at the Beckman Institute for Advanced Science and Technology, University of Illinois, Urbana-Champaign) and PyMOL Molecular Graphics System v2.5.7[30] (Schrödinger, LLC, New York City, NY, USA). Additionally, UCSF Chimera v1.17.3 (developed by the Resource for Biocomputing, Visualization, and Informatics at the University of California, San Francisco, with support from NIH P41-GM103311.) was employed in the visualization process.

RESULTS AND DISCUSSION

Results

Aptamer selection and optimization

In **(Table 1)**, the docking scores obtained from HDOCK docking tool are listed. Some structures, such as seq 4 and seq 7, have relatively high MFE suggesting structural instability. Among the selected sequences, seq 6 with the length of 46-mer and GC content of 45.6% was the best-binding structure, and exhibited the lowest docking score (score: -311.39).

Since seq 6 had a relatively high free energy of (-4.6 kcal/mol), it was optimized to obtain a more stable structure. The last five nucleotides at both the 5' and 3' ends of the sequence were designed to be complementary with each other. and random mutations were introduced to generate ten new sequences.

As shown in **(Table 2)**, certain structures like seq 6-1, seq 6-5, and seq 6-8 exhibit relatively high MFE, suggesting structural instability. Three structures (seq 6-2, seq 6-3, seq 6-9) showed higher binding scores and

more stable complexes compared to the original structure, suggesting that the minor nucleotide variations can improve the stability of the aptamer and its binding properties, and this can be further evaluated by in vitro experiments[31]. Seq 6-9 demonstrated the best binding affinity and 2d best MFE (score: -358.56; MFE: -20.40 kcal/mol), so it was optimized by introducing additional mutations, and three new sequences were generated **(Table 3).**

Table 1: Docking scores and free energy values for the top five aptamer sequences.

Code	Sequence (5′–3′)	Length (bp)	CG%	MFE (kcal/mol)	Docking score
seq 1	CUCACGCGUGGUUUCCACUACUUUCUUC CAGUCGCACCCCUAAUAAGUCG	50	52	-4.00	-271.51
seq 6	GGUCAUCAAGUUAGUCAAACCAGCGAC GACGGUGUAGCAUAGUAUU	46	45.6	-4.60	-311.39
seq 40	AUAUCCAGCCUACAACAAACCGCGCAAG GACAUUACCUUUCCAGCUG	47	48.9	-3.90	-306.79
seq 77	GUCACGCGUGUUUCCACUACUUUCUUCC AGUCGCACCCCUAAUAACCUGA	50	50	-1.50	-289.44
seq 92	UACCUAAUUGUUGUCCUAAUCAAGUAC ACGUGGACGCUGAACCUCUUU	48	41.6	-4.70	-304.43

MFE: minimum free energy.

Table 2: New Sequences generated by introducing mutations in seq-6 aptamer.

Code	Sequence (5′–3′)	CG%	MFE (kcal/mol)	Docking score
seq 6-1	GGAUCGGUCAUCAAGUUAGUCAAACCAGCGAC GACGGUGUAGCAUAGUAUUGAUCC	48.2	-11.10	-296.80
seq 6-2	GGAUCGGU_AUCAAGUUAGUCAAACCAGCGACG ACGGUUUAGCAUAGUAUUGAUCC	44.6	13.80	-322.92
seq 6-3	GGAUCGGU_AUCAAGUUAGUCAAACCAGCGACG ACGGUUUAGCAUAGUACCGAUCC	48.2	18.40	-317.03
seq 6-4	GGAUCGGUGACCAAGUUAGUCAAACCAGCGAC GACGGUUUAGCAUAGUGAUUGAUCC	49.1	-14.70	-301.82
seq 6-5	GGAUCGGUCAUCAAGUUAGUCAAACCAGCGAC GACGGUUUAGCAUAGUAUUGAUCC	46.4	-10.00	-301.76
seq 6-6	GGAUCGGUCAUCAACUUAGUCAAACCAGCGAC GACGGUUUAGCAUAGUAUUGAUCC	46.4	13.10	-300.33
seq 6-7	_GGUCGGU_AUCAAGUUAGUCAAACCAGCGACG ACGGUUUAGCAUAGUACCGACC_	48.2	-17.10	-300.62
seq 6-8	GGAU_G_UCAUCAAGUUAGUCGGAUUCCUAUU_ ACGACGGUGUAGCAUAGUAUUGAUCC	40.6	-6.60	-262.05
seq 6-9	GGAUCGGUGGCCAAGUUAGUCAAACCAGCGAC GACGGUUUAGCAUAGCCCCGAUCC	57.1	-20.40	-358.56
seq 6-10	GGAUCGGUGGCCAAGUUAGUGAAACCAGCGAC GACGGUUGGGUAGCAUAGCCCCGAUCC	59.3	-22.90	-310.93

Table 3: New Sequences generated by introducing mutations in seq 6-9 aptamer.

Code	Sequence	length	CG%	MFE
Seq 6-9-1	GGAUCGGUCAUCAAGUUAGUCAAACCAGCGACGA CGGUGUAGCAUAGUAUUGAUCC	56	55.3	-20.30
seq 6-9-2	GGAUCGGU_AUCAAGUUAGUCAAACCAGCGACGAC GGUUUAGCAUAGUAUUGAUCC	58	58.6	-20.40
seq 6-9-3	GGAUCGGUGGCCAAGUUAGUCAAACC_CCGUGUGC CGGUUUAGCAUAGCCCCGAUCC	56	58.9	-20.00

The generated sequences were further examined using the RNAfold web server 2.6.3 for secondary structures prediction. The overall topologies of the secondary structures of the three aptamers were identical **(Fig. 1 A)**. The Vienna Formula, (((((((.((...(((....((((.....)))))))))) ...))))))))) and (((((((.(((...((((....((((.... .))))))))...))))))))))) and (((((((.(((...((((....((((. ... .))))))))))...)))))))), remained consistently in the same sequential order. The secondary structures of the three aptamers consist of four stems, a hairpin loop, an inner loop, two bulging loops, Watson–Crick base pairing 31, and wobble base pairing (guanine-uracil (G-U)) (1-2) **(Fig. 1A)**. The high number of Watson-Crick base pairing maintains the conformation of the aptamer during docking[32].

The secondary structures of aptamers are due to intramolecular nucleotide base pairing, which allows the molecule to fold in specific conformation 13 . They are also affected by temperature and ionic concentrations[33].

The RNA sequences and the dot-bracket secondary structure notations were input into the RNA Composer server to build the 3D model. The tertiary structures exhibited a remarkable degree of conformity **(Fig. 1C).** However, the binding properties of an aptamer to its target are related to its structure 7. The three-dimensional structures of the aptamers can be attributed to the flexibility of the phosphodiester backbones of aptamers which confers different torsional angles, and allows the generation of a wide range of 3D structures[33].

MDockPP is an Online Server renowned for providing structure predictions for diverse complexes such as protein-protein, protein-RNA, and protein-DNA. The docking algorithm is grounded in Fast Fourier Transform (FFT), utilizing a 6-degree rotational angle interval. It is powered by the University of Missouri (https://zougrouptoolkit.missouri.edu/MDockPP/)[34].

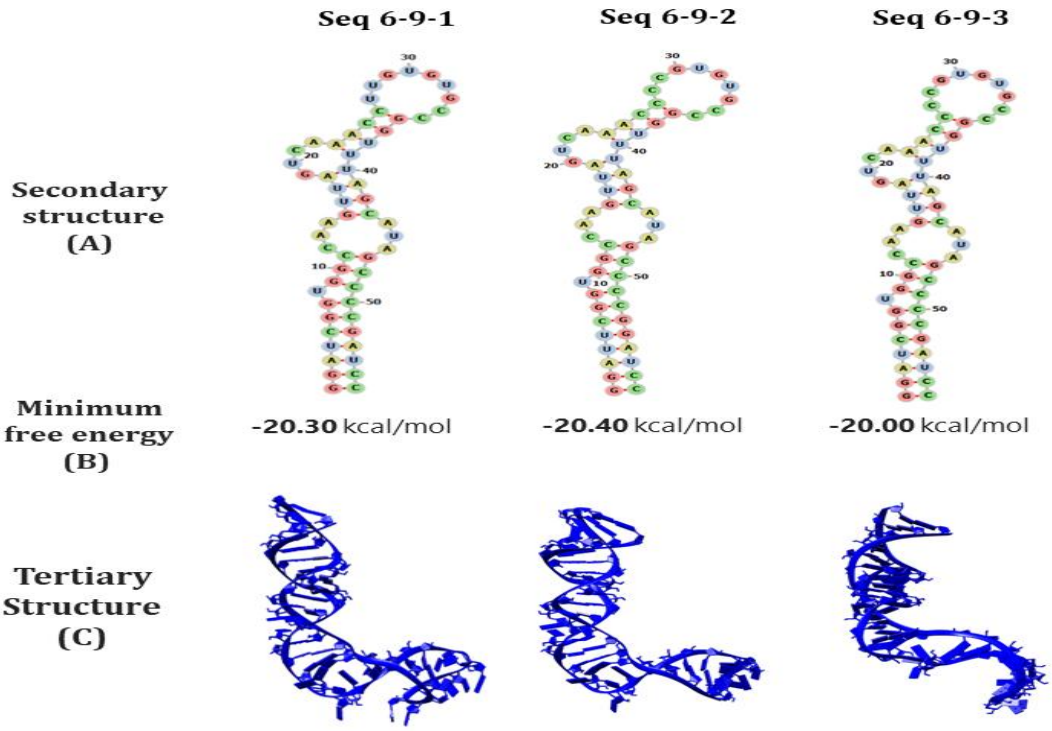

Fig. 1: The RNA secondary structures of the RNA aptamers, (B): the corresponding minimum free energy (MFE), (C): The tertiary structures.

NPdock (Nucleic acid-Protein Dock) is a server for modeling of DNA-protein and RNA-protein complexes (https://genesilico.pl/NPdock/). It combines GRAMM for global macromolecular docking, scoring with a statistical potential, clustering of best-scored structures, and local refinement. This server is maintained by the Laboratory of Bioinformatics and Protein Engineering at the International Institute of Molecular and Cell Biology in Warsaw. **Fig. 2.** Shows the surface view of the NPdock generated aptamer-AFP complexes[35].

Nine docking experiments were performed to predict the most likely aptamer for emerging as AFP aptamer. The binding affinities in the resulting complexes were estimated using Z_T scores **(Table 4)**. We obtained a Z_T value of -5.38, -5.6, and -6.66 for seq 6-9-1, seq 6-9-2, and seq 6-9-3 respectively.

Protein–aptamer interaction

The interaction of the three mutant RNA sequences with the target (AFP) was identified using the PLIP web server **(Table 5)**. The detailed report obtained from PLIP serves as a comprehensive documentation of the molecular interactions between the aptamer and the protein. Such information can be used in further optimization of the aptamer for improved binding affinity for experimental studies.

Table 4: Z-score values of docking AFP- RNA aptamer complexes.

Code	HDOCK (Zh-score)	NPdock (Zn-score)	MDockPP (Zm-score)	Total (Zt-score)
Seq 6-9-1	-1.32	-1.66	-2.4	-5.38
seq 6-9-2	-1.51	-2.26	-1.83	-5.6
seq 6-9-3	-1.33	-2.82	-2.51	-6.66

Table 5: Analysis of the predicted interactions in the selected aptamer-AFP complex.

PLIP									
	NPdock pose			MdockPP pose			Hdock pose		
	NHI	NHB	NSB	NHI	NHB	NSB	NHI	NHB	NSB
Seq 6-9-1	3	24	6	2	20	8	-	24	8
Seq 6-9-2	5	38	6	4	31	10	-	17	6
Seq 6-9-3	5	36	9	2	23	5	-	21	8

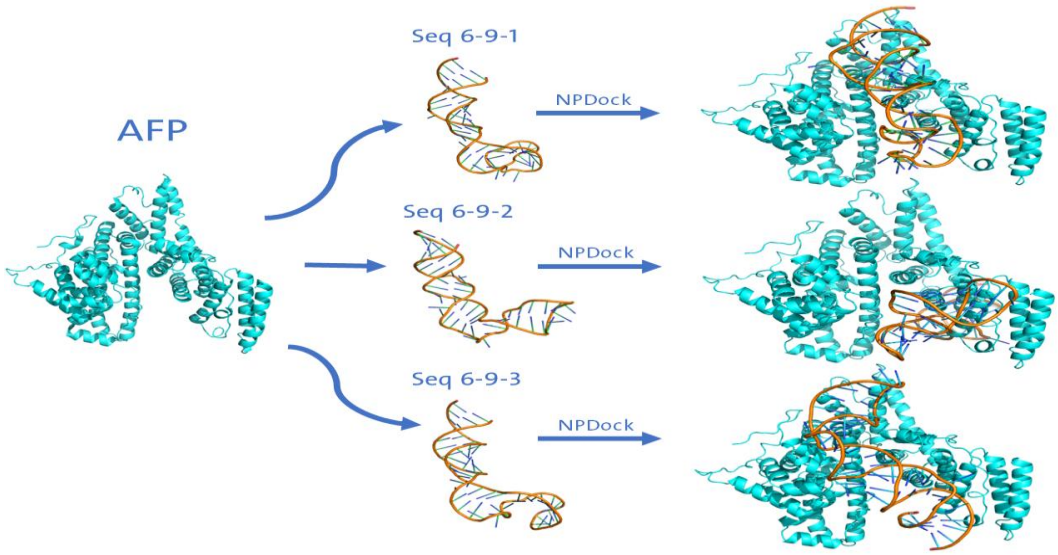

Fig. 2: Surface view of the NPdock generated aptamer-AFP complexes. The blue color represents the target (AFP) while the brown color represents the aptamer.

Overall, the highest number of interactions were reported in NPdock generated aptamer-AFP complexs, with a total of 33, 49, and 50 predicted interactions for seq 6-9-1 and seq 6-9-2 and seq6-9-3 aptamer–protein complexes, respectively.

Taken together, the in silico predictions (Z_T score and the predicted interactions) suggest that the selected RNA aptamer (seq 6-9-3) can emerge as an aptamer to the AFP. Therefore, this aptamer was selected for further analysis.

Aptamers recognize specific epitopes on the protein surface to bind it 36. These are predominantly electropositive and dominated by polar interactions, H-bonds, and charge-charge interactions 33. It is assumed that the aptamer-protein interactions begin with the formation of electrostatic interactions with a protruded surface of the protein, thus establishing initial contact with RNA aptamers[36].

Table S1 presented detailed information about the amino acid-base interactions in the NPdock generated seq 6-9-3 aptamer-AFP complex.

Hydrogen bonding (H-bond) was the most common surface interaction between the seq 6-9-3 aptamer and the target AFP. H- bonds are one of the strongest interactions, and the affinity between the aptamer and its target is related to the number and distance of these bonds 7. Many hydrogen bonds (36 bonds) were identified in the seq 6-9-3 aptamer-AFP complex interactions. Apart from hydrogen bonding, the hydrophobic interactions (HI) also play an important role in keeping the aptamer inside the binding pocket of the protein 32. Five hydrophobic bonds were identified in the AFP–aptamer interactions, including 445SER/49C, 487ARG/11C, 534HIS/53A, 536ASP/54U, and 554ILE/50C.

Additionally, salt bridges interaction plays a major role in stabilizing the RNA−protein interfaces[36]. Salt bridge interactions were identified at 9 interaction sites in seq 6-9-3 aptamer-AFP complex. Phosphate and guanidine groups of RNA were involved in the formation of salt bridge with amino acids.

Three binding interfaces can be recognized in the aptamer **(Fig. 3).** The first binding interface (the first stem, the first bulge loop, and the second stem) was highly involved in hydrogen bonding with the protein with 27 hydrogen bonds, 15 of which were in the first bulge loop. Four hydrophobic interactions and six salt bridges were also identified in this interface **(Fig. 3A)**. In the second binding interface (the internal loop), 5 hydrogen bonds, one hydrophobic interaction, and two salt bridges were identified **(Fig. 3B).** Whereas only a few interactions were identified in the third binding interface (the third stem, the second bulge loop, the fourth stem, and the hairpin loop), including four hydrogen bonds and one salt bridge **(Fig. 3C).**

Some nucleotides formed more than one bond, such as U54 with 3 hydrogen bonds with 535 LYS, 536 ASP, and 589 GLU, a hydrophobic bond with 536 ASP, and two salt bridges with 534 HIS and 535 LYS; C50 with 6 hydrogen bonds with 444 SER, 445 SER, 452 ARG, 550 GLN, and two with 551 GLN, and a hydrophobic bond with 554 ILE; C49 with 4 hydrogen bonds with 444 SER, 445 SER, 447 LEU and 448 MET, and a hydrophobic bond with 445 SER; A53 with a hydrogen bond with 532 ILE, a hydrophobic bond with 534 HIS, and a salt bridge with 534 HIS; U8 with three hydrogen bonds, two with 525 ALA and one with 527 SER; G10 with two hydrogen bonds with 443 THR and 487 ARG, and a salt bridge with 446 GLU and 11 C with three hydrogen bonds with 493 VAL, 487 ARG, and 491 THR, a hydrophobic bond with 487 ARG, and a salt bridge with 487 ARG. **Fig. 4**. shows the amino acid–base interactions in the NPdock generated aptamer (seq 6-9-3) -AFP complex.

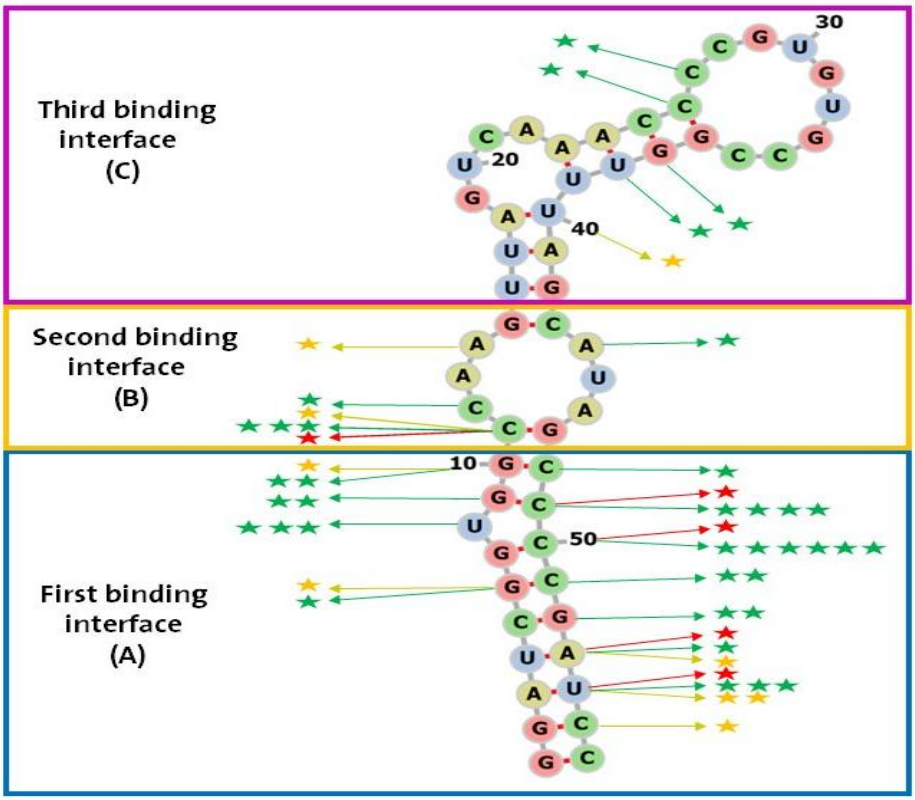

Fig. 3: Three binding interfaces in the seq 6-9-3 aptamer. Hydrogen bonds (green stars), hydrophobic bonds (red stars) and salt bridge (yellow stars).

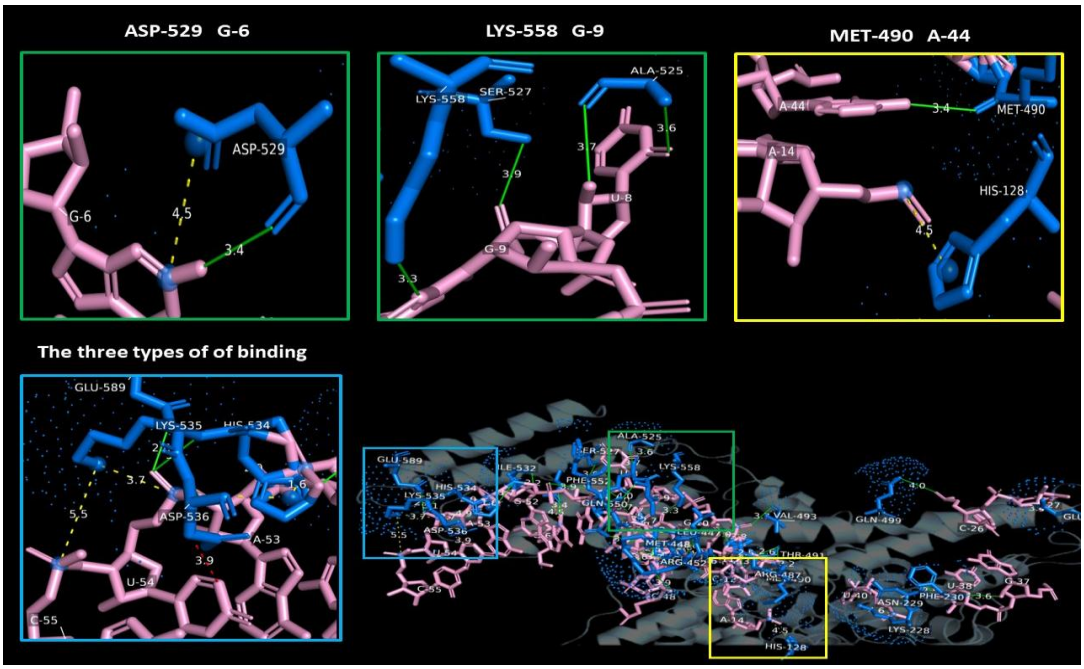

Fig. 4: 3D view shows the amino acid-base interactions in the NPdock generated aptamer (seq 6-9-3) - AFP complex, including hydrogen bonds (green line), salt bridges (yellow dash-dot line), and hydrophobic interactions (red dash-dot line.)

Some amino acids also formed more than one bond, such as 444 SER formed 3 hydrogen bonds: one each with 9 G, 49 C, and 50 C. Furthermore, 445 SER formed 3 hydrogen bonds with 48 C, 49 C, and 50 C , along with a hydrophobic bond with 49 C. Amino acid 487 ARG engaged in two hydrogen bonds with 10 G and 11 C, a hydrophobic bond with 11 C, and a salt bridge with 11 C. 534 HIS formed a hydrophobic bond with 53 A and two salt bridges with 53 A and 54 U. Lastly, 535 LYS formed a hydrogen bond with 54 U and two salt bridges with 54 U and 55 C.

The interacting residues identified in our study were analyzed for consistency with the literature. The binding interface of the AFP protein with different molecules was predicted in previous reports via molecular docking. Molecular docking of AFP with caspase-3 revealed that AFP protein could interact with caspase-3 through specific amino acids (Ser-135, Lys-161, Arg-168, Arg-214, Ser-445, Arg-452, Lys-558)[37]. The individual residues (Asp-529, Met-490, Lys-107, Ser-135, Leu-105, Glu-106) were shown to be involved in the binding interface of AFP and phosphatase and tensin homolog (PTEN)[38]. The residues (Ser-445, Met-448, Arg-452, Met-548, and Glu-551, Leu-138) were shown to be involved in the binding interface of AFP and diethylstilbestrol (DES)[39] The interacting residues that were identified in our study and are in agreement with the literature are shown in **Fig. 5**.

Molecular Dynamic simulation

MD simulation is an imperious part of computational analyses. It offers detailed information about the interaction between ligand and protein, with a dynamic perspective[40]. Therefore, ntending to achieve molecular insights into the self-conformational perturbations that the protein brings to achieve stability and flexibility with the selected aptamer, we allowed the best protein-aptamer complex to undergo MD simulation for a time period of 32.5 ns. The RMSD, H-bonds, RMSF and Rg were determined to have deeper knowledge about the stability, flexibility of the residues and the compactness of seq9-3 aptamer/AFP complex.

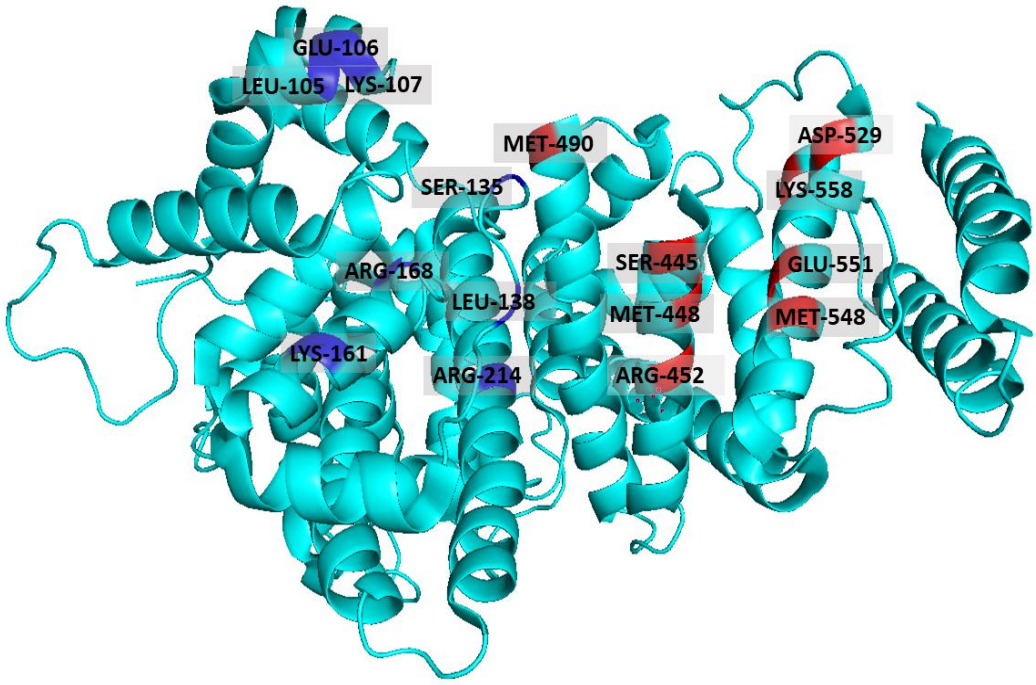

Fig. 5: The interacting residues identified in the AFP protein according to the literature (highlighted in blue). The residues identified in our study that agreed with the literature are highlighted in red.

Root Mean Square Deviation (RMSD)

The conformational stability of the seq9-3 aptamer/AFP complex was analyzed by plotting RMSD. RMSD determines the average change in displacement of specific atoms for a specific frame with respect to a reference frame[41]. Low levels of RMSD, with consistent fluctuations throughout the entire simulation indicate stability of the system. The highly deviated RMSD values can also indicate major conformational transitions that have occurred in the protein to get stable conformation with the ligand[40].

Fig. 6 displays the RMSD value of the seq9-3 aptamer/AFP complex with respect to time. The highest RMSD value was 7.97 A, and the average RMSD was 6.19±1.21 A. The RMSD graph of seq9-3 aptamer/AFP complex showed an upward trend from 1.23 to 7.97 Å throughout the first 9.82 ns. After 13 ns, the RMSD pattern showed a fluctuating trend but was slightly stable as compared to the first 10 ns of the simulated trajectory. The complex reached a short-term steady state from 18.54 to 20.42 ns in the simulation, with an average of 6.05 A, and then suddenly increased to 7.48 Å at 22.14 ns.

After 24.06 ns, the RMSD pattern stabilized with an average of 6.5 A until the end of the simulation. These findings indicate that the aptamer remained sufficiently bound to the AFP throughout the simulation, and the complex obtained a stable conformation.

Root Mean Square Fluctuation (RMSF)

The RMSF parameter is effective for assessing the local flexibility in a protein structure and detecting the rigid and flexible regions[42]. RMSF analyzes a particular segment of a protein that deviates from its mean structure, which usually occurs upon ligand interaction. Residues that display higher RMSF values indicate increased flexibility, whereas lower RMSF values indicate lesser flexibility [40], and have a relatively more number of H-bonds for stability[43].

The RMSF of the seq 6-9-3 aptamer/AFP simulated complex was analyzed **(Fig. 7).** The RMSF graph represented the residues on the x-axis, and the fluctuation values on the y-axis. The highest and lowest RMSF values were 10.22 Å and 0.67 Å, respectively, and the average RMSF was 1.52±0.96 Å.

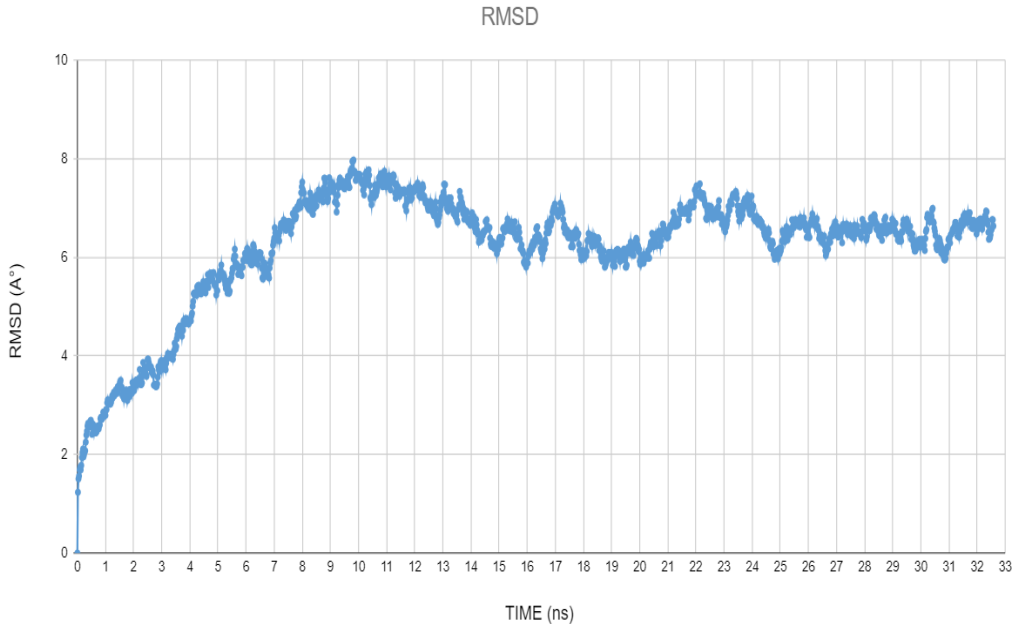

Fig. 6: RMSD plot of the seq9-3 aptamer/AFP complex during the MD simulation.

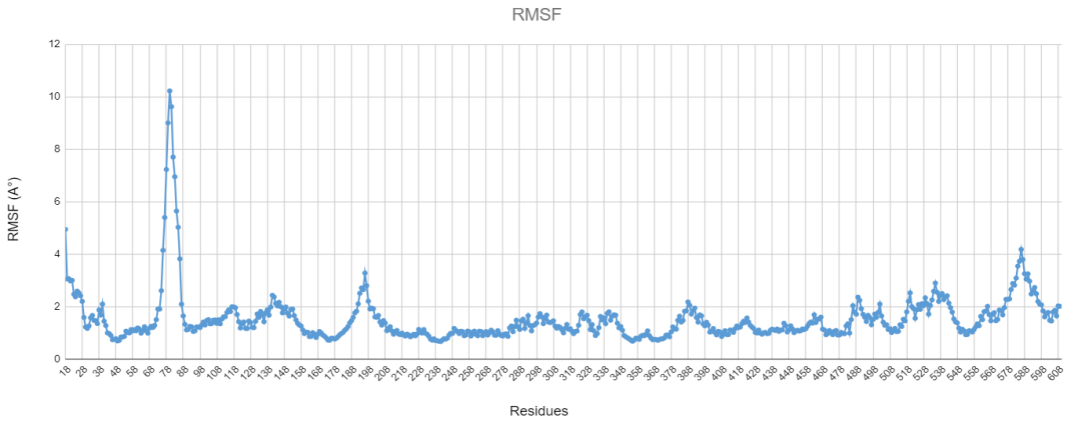

Fig. 7: RMSF plot of the seq6-9-3 aptamer/AFP complex. RMSF was calculated for Cα atoms *of the protein.*

It can be observed from the RMSF plot that some residues display large changes, particularly the residues in the range of 77 to 85 (RMSF values between 5–10.22 Å), which are located in the protein's loop region, and the residue 18 SER (RMSF: 4.94 Å) which is located in the protein's terminal region. These significant fluctuations of RMSF values were observed for the residues of amino acids not bound to the aptamer. However, α- helices and ß-strands are often more rigid than the unstructured portion of a protein, and more stable than loop regions[44]. It is also predictable that RMSF values in the terminal part of a protein structure will be higher than those in the in-between part since these sites fluctuate more than other sites[45].

To investigate whether the complex is stable, we observed the RMSF plot at specific residues of the AFP protein where interaction occurs. The RMSF profile showed that the residues of amino acids bound to the aptamer did not show significant fluctuations during the MD simulation, and had lower RMSF than 2.58 Å, except for the Lys535 (RMSF:2.89 Å), indicating stable and low flexibility of the complex.

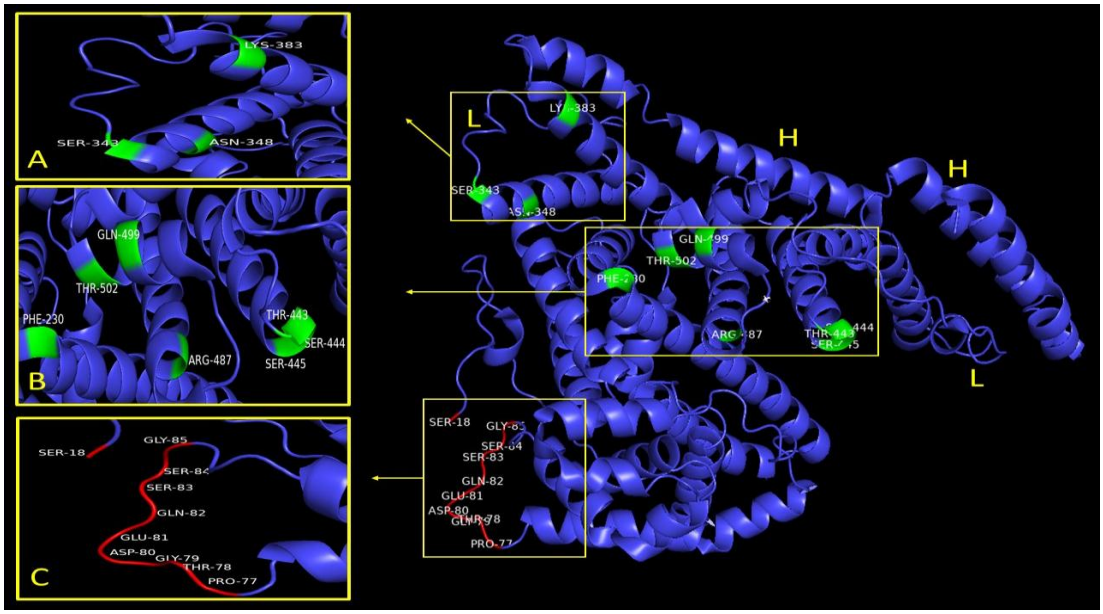

Fig. 8: 3D cryo-EM structure of human AFP. H represents the alpha helices, and L represents the loops. (A, B): Interacting residues in the seq 6-9-3 aptamer/AFP complex (highlighted in green), C: non-interacting residues that exhibit high RMSF values.

The radius of gyration (Rg)

Rg parameter is effective to assess the compactness and structural integrity of the studied system[46]. It determines the mass distribution around the center of mass of the protein, and offers insight into the conformational changes of the protein over time. By quantifying the Rg parameter at different time points through a simulation, the contraction or expansion of the protein structure, and the fluctuations in its shape can be assessed[43].

Fig. 9 displays the Rg plot of the seq 6-9-3 aptamer/ AFP complex. Rg-time fluctuations were maintained between 27.08 Å and 28.34 Å throughout 32.58 ns with an average value of 27.62±0.20 Å. This result provides a clear evidence of minimal changes in the conformational state of the protein, and showed that the protein structure was condensed throughout the 32.58 ns run.

Hydrogen bonds (H-bond) analysis

To gain further insights into the binding of the selected aptamer to the target AFP during simulation, the H-bond were also monitored. H-bond is polar bond formed by the interaction of a hydrogen atom that is covalently bonded to an electronegative atom (donor) with another electronegative atom (acceptor). The study of the intermolecular interaction by hydrogen bonds offers information about the amino acids involved in stabilizing of protein structure 32. The number of H-bonds can be used as an indicator to determine the stability of aptamer-protein interaction[47]. The total number of H-bonds that appeared in the MD simulation trajectories for the seq9-3 aptamer/AFP complex is shown in **(Fig. 10)**.

The complex had an average of 8.52±4.10 hydrogen bonds, with the highest number of 35 bonds at the start of the simulation and the lowest number of 1 H-bond in the trajectory. At 32.58 ns, the final number of hydrogen bonds between the AFP protein and seq9-3 aptamer was 6. In the last frame of the MD simulation for the complex, hydrogen bonds appeared in 535LYS/53A, 230 PHE/25C, 348ASN/ 27C, 535LYS/52G, 529ASP/6G, 530LYS/7G, 532ILE/9G and salt bridges appeared in 530LYS/8U, 530LYS/9G **(Fig. 11).** The H-bonds formation between the protein and the aptamer showed that they had a stable and strong binding. Table S2. presents detailed data about the interactions and occupancy percentages of hydrogen bonds for the seq9-3 aptamer/AFP complex during the simulation. ARG487 and LYS530, which are polar and positively charged residues, were the most important amino acids because their side chains could form hydrogen bonds with the aptamer, with high occupancy rates, such as (LYS530/G9:22.39%, LYS530/G7:22.02%, LYS530/G7:19.45%, LYS530/G9:16.81%, LYS530/G9:14.48%, LYS530/G7:11.29%, LYS530/G9:10.80%, ARG487/C11:34.05%, ARG487/C12: 27.06%, ARG487/C12:18.71%). In addition, they could form H-bonds with other nucleotides of the aptamer with moderate or low occupancy rates.

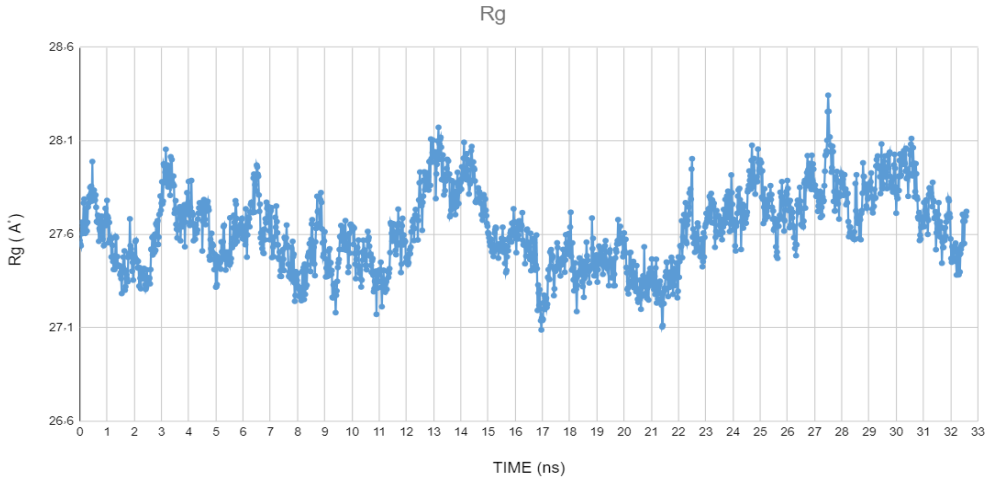

Fig. 9: Rg plot of the seq6-9-3 aptamer/AFP complex during the MD simulation.

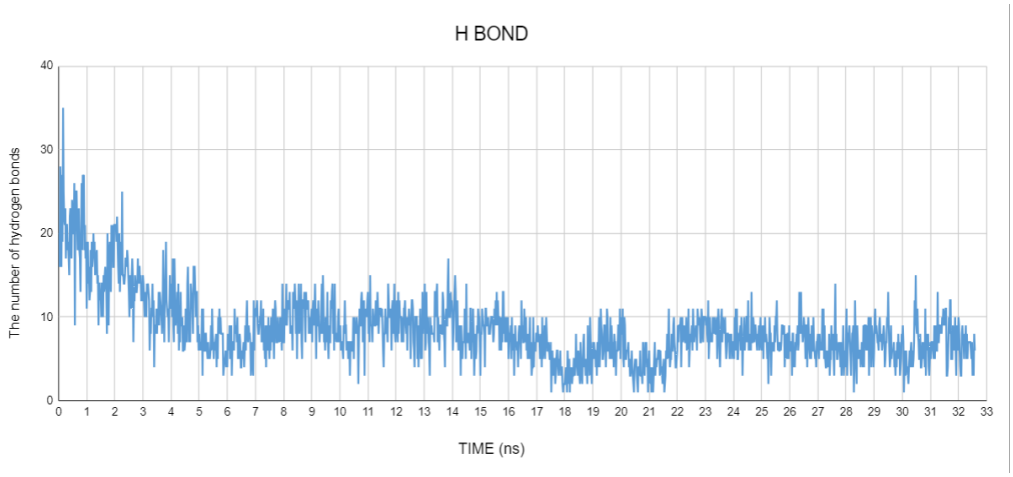

Fig. 10: Number of hydrogen bonds of the seq9-3 aptamer/AFP complex during the 32.58 ns MD simulation.

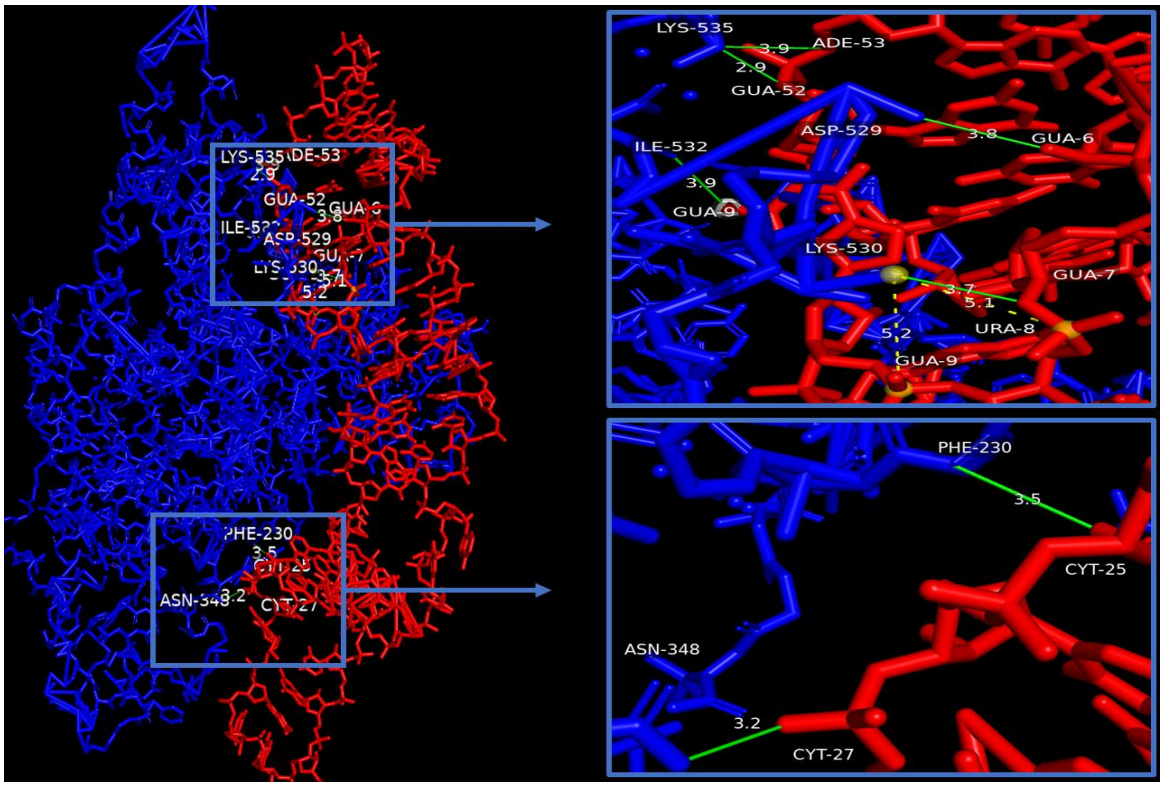

Fig. 11: Visualization of the H-bonds formed by the the seq9-3 aptamer and AFP protein in the last frame of MD simulation. The aptamer is colored in red, the AFP protein is colored in blue, H-bonds shown by green lines and salt bridges shown by yellow.

Discussion

In this study, one hundred random RNA sequences were generated. Their 3D structures were docked with the AFP. The aptamer sequence with the best docking score was selected, and random mutations were introduced in its sequence to get a more stable structure with high affinity. After multiple rounds of mutations, the three selected mutant sequences (seq 6-9-1, seq 6-9-2, seq 6-9-3) were examined using the RNAfold server for secondary structures prediction. The secondary structures of the three aptamers consist of four stems, a hairpin loop, an inner loop, two bulging loops, Watson–Crick base pairing, and wobble base pairing (guanine-uracil (G-U)) (1-2) **(Fig. 1A)**. The high number of Watson-Crick base pairing maintains the conformation

of the aptamer during docking[31,32]. The secondary structures of aptamers are due to intramolecular nucleotide base pairing, which allows the molecule to fold in specific conformation[13]. They are also affected by temperature and ionic concentrations[33].

The tertiary structures of the mutant sequences were docked to the AFP using different docking platforms (HDOCK, MdockPP, and NPdock). Three different docking servers have been used to verify the binding affinity of the aptamer-protein complex, and to actually be able to choose the aptamer with the highest binding affinity

HDOCK is a web server for protein-protein and protein-DNA/RNA docking, based on a hybrid algorithm that combines template-based modeling and ab initio-free docking. It plays an important role in facilitating the exploration of molecular interactions between proteins and nucleic acids. HDOCK was developed by Huang Laboratory.

MDockPP is an Online Server renowned for providing structure predictions for diverse complexes such as protein-protein, protein-RNA, and protein-DNA. The docking algorithm is grounded in Fast Fourier Transform (FFT), utilizing a 6-degree rotational angle interval. It is powered by the University of Missouri (https://zougrouptoolkit.missouri.edu/MDockPP/)[34].

NPdock (Nucleic acid-Protein Dock) is a server for modeling of DNA-protein and RNA-protein complexes (https://genesilico.pl/NPdock/). It combines GRAMM for global macromolecular docking, scoring with a statistical potential, clustering of best-scored structures, and local refinement. This server is maintained by the Laboratory of Bioinformatics and Protein Engineering at the International Institute of Molecular and Cell Biology in Warsaw. **Fig. 1 B**. Shows the surface view of the NPdock generated aptamer-AFP complexes[35].

Based on Z_T score and the predicted interactions, the RNA aptamer (seq 6-9-3) was selected as a potential aptamer to the AFP. It showed the highest number of interactions with the protein. Aptamers recognize specific epitopes on the protein surface to bind it[36]. These are predominantly electropositive and dominated by polar interactions, H-bonds, and charge-charge interactions[33]. It is assumed that the aptamer-protein interactions begin with the formation of electrostatic interactions with a protruded surface of the protein, thus establishing initial contact with RNA aptamers[36].

Hydrogen bonding (H-bond) was the most common surface interaction between the seq 6-9-3 aptamer and the target AFP. H- bonds are one of the strongest interactions, and the affinity between the aptamer and its target is related to the number and distance of these bonds[7]. Many hydrogen bonds (36 bonds) were identified in the seq 6-9-3 aptamer-AFP complex interactions. Apart from hydrogen bonding, the hydrophobic interactions (HI) also play an important role in keeping the aptamer inside the binding pocket of the protein[32]. Five hydrophobic bonds were identified in the AFP–aptamer interactions, including 445SER/49C, 487ARG/11C, 534HIS/53A, 536ASP/54U, and 554ILE/50C.

Additionally, salt bridges interaction plays a major role in stabilizing the RNA−protein interfaces[36]. Salt bridge (SB) interactions were identified at 9 interaction sites in seq 6-9-3 aptamer-AFP complex. Phosphate and guanidine groups of RNA were involved in the formation of salt bridge with amino acids.

The interacting residues identified in our study were analyzed for consistency with the literature. The binding interface of the AFP protein with different molecules was predicted in previous reports via molecular docking. Molecular docking of AFP with caspase-3 revealed that AFP protein could interact with caspase-3 through specific amino acids (Ser-135, Lys-161, Arg-168, Arg-214, Ser-445, Arg-452, Lys-558)[37]. The individual residues (Asp-529, Met-490, Lys-107, Ser-135, Leu-105, Glu-106) were shown to be involved in the binding interface of AFP and phosphatase and tensin homolog (PTEN)[38]. The residues (Ser-445, Met-448, Arg-452, Met-548, and Glu-551, Leu-138) were shown to be involved in the binding interface of AFP and diethylstilbestrol (DES)[39]

MD simulation is an imperious part of computational analyses. It offers detailed information about the interaction between ligand and protein, with a dynamic perspective[40]. To achieve molecular insights into the self-conformational perturbations that the protein brings to achieve stability and

flexibility with the selected aptamer, we allowed the best protein-aptamer complex to undergo MD simulation for a time period of 32.5 ns. The RMSD, H-bonds, RMSF and Rg were determined to have deeper knowledge about the stability, flexibility of the residues and the compactness of seq9-3 aptamer/AFP complex.

The conformational stability of the seq9-3 aptamer/AFP complex was analyzed by plotting RMSD. RMSD determines the average change in displacement of specific atoms for a specific frame with respect to a reference frame[41]. Low levels of RMSD, with consistent fluctuations throughout the entire simulation indicate stability of the system. The highly deviated RMSD values can also indicate major conformational transitions that have occurred in the protein to get stable conformation with the ligand[40].

The RMSD pattern stabilized with an average of 6.5 A, which indicates that the aptamer remained sufficiently bound to the AFP throughout the simulation, and the complex obtained a stable conformation.

The RMSF parameter is effective for assessing the local flexibility in a protein structure and detecting the rigid and flexible regions[42]. RMSF analyzes a particular segment of a protein that deviates from its mean structure, which usually occurs upon ligand interaction. Residues that display higher RMSF values indicate increased flexibility, whereas lower RMSF values indicate lesser flexibility[40], and have a relatively more number of H-bonds for stability[43].

It can be observed from the RMSF plot of the seq 6-9-3 aptamer/AFP that some residues display large changes, particularly the residues in the range of 77 to 85 (RMSF values between 5–10.22 Å), which are located in the protein's loop region, and the residue 18 SER (RMSF: 4.94 Å) which is located in the protein's terminal region **(Fig. 5).** These significant fluctuations of RMSF values were observed for the residues of amino acids not bound to the aptamer. However, α- helices and ß-strands are often more rigid than the unstructured portion of a protein, and more stable than loop regions[44]. It is also predictable that RMSF values in the terminal part of a protein structure will be higher than those in the in-between part since these sites fluctuate more than other sites[45].

To investigate whether the complex is stable, we observed the RMSF plot at residues of the AFP protein where interaction occurs. The RMSF profile showed that the residues of amino acids bound to the aptamer did not show significant fluctuations during the MD simulation, and had lower RMSF than 2.58 Å, except for the Lys535 (RMSF:2.89 Å), indicating stable and low flexibility of the complex.

Rg parameter is effective to assess the compactness and structural integrity of the studied system[46]. It determines the mass distribution around the center of mass of the protein, and offers insight into the conformational changes of the protein over time. By quantifying the Rg parameter at different time points through a simulation, the contraction or expansion of the protein structure, and the fluctuations in its shape can be assessed[43].

The Rg plot of the seq 6-9-3 aptamer/ AFP complex provides a clear evidence of minimal changes in the conformational state of the protein, and showed that the protein structure was condensed throughout the 32.58 ns run.

To gain further insights into the binding of the selected aptamer to the target AFP during simulation, the H-bond were also monitored. H-bond is polar bond formed by the interaction of a hydrogen atom that is covalently bonded to an electronegative atom (donor) with another electronegative atom (acceptor). The study of the intermolecular interaction by hydrogen bonds offers information about the amino acids involved in stabilizing of protein structure[32]. The number of H-bonds can be used as an indicator to determine the stability of aptamer-protein interaction[47].

The H-bonds formation in the seq9-3 aptamer/AFP complex showed that they had a stable and strong binding. ARG487 and LYS530, which are polar and positively charged residues, were the most important amino acids because their side chains could form hydrogen bonds with the aptamer, with high occupancy rates, such as (LYS530/G9:22.39%, LYS530/G7:22.02%, LYS530/G7:19.45%, LYS530/G9:16.81%, LYS530/G9:14.48%, LYS530/G7:11.29%, LYS530/G9:10.80%, ARG487/C11:34.05%,

ARG487/C12: 27.06%, ARG487/C12:18.71%). In addition, they could form H-bonds with other nucleotides of the aptamer with moderate or low occupancy rates.

Conclusions

In the current study, an RNA aptamer was selected and optimized through a non-SELEX *in silico* method, which is simple and cost-effective method that does not require sophisticated instruments. The selected seq 6-9-3 aptamer showed a relatively stable structure and good binding affinity to the target AFP. Therefore, this aptamer could serve as a good candidate for the diagnosis and treatment of HCC. However, further *in vitro* and *in vivo* studies are needed before a final conclusion can be reached.

Acknowledgements

The authors are grateful to Eng. Joseph SHENEKJI, faculty of Biotechnology Engineering for his help and support in the data analysis.

Abbreviations

AFP: Alpha-fetoprotein
Cryo-EM: cryo-electron microscopy
H-bonds: hydrogen bond
HCC: Hepatocellular carcinoma
HI: hydrophobic interactions
MD: Molecular dynamics
MFE: minimum free energy
PDB: RCSB Protein Data Bank
PLIP: Protein-Ligand Interaction Profiler
RMSD: root-mean-square deviation
RMSF: root-mean-square fluctuation
Rg: radius of gyration
SB: salt bridge
SELEX: Systematic evolution of ligands by exponential enrichment.

REFERENCES

1. Z. Wei, Y. Zhang, H. Lu, J. Ying, H. Zhao and J. Cai, "Serum alpha-fetoprotein as a predictive biomarker for tissue alpha-fetoprotein status and prognosis in patients with hepatocellular carcinoma", ***Transl Cancer Res,*** 11(4), 669–677 (2022)
2. C. O. M. Jasirwan, A. Fahira, L. Siregar and I. M. Loho, "The alpha-fetoprotein serum is still reliable as a biomarker for the surveillance of hepatocellular carcinoma in Indonesia", ***BMC Gastroenterol,*** 20(1), 215 (2020).
3. A. T. K. Koshvandi, "Recent advances in optical biosensors for the detection of cancer biomarker α-fetoprotein (AFP)", ***TrAC Trends Anal Chem,*** 128, 115920 (2020).
4. O. O. Adigun, S. N. S. Yarrarapu, M. Zubair and S. Khetarpal, "Alpha Fetoprotein", ***in StatPearls,*** (2023).
5. J. Głowska-Ciemny, M. Szymański, A. Kuszerska, Z. Malewski, C. Von Kaisenberg and R. Kocyłowski, "The Role of Alpha-Fetoprotein (AFP) in Contemporary Oncology: The Path from a Diagnostic Biomarker to an Anticancer Drug", ***Int J Mol Sci,*** 24(3), 2539 (2023).
6. Y. J. Lee and S.-W. Lee, "Regression of hepatocarcinoma cells using RNA aptamer specific to alpha-fetoprotein", ***Biochem Biophys Res Commun***, 417(1), 521–527 (2012).
7. H. Zhang, C. Lv, Z. Li, S. Jiang, C. Dan, S. B. Liu, *et al.*, "Analysis of aptamer-target binding and molecular mechanisms by thermofluorimetric analysis and molecular dynamics simulation", ***Front Chem,*** 11, 1144347 (2023).
8. S. S. S. Toloun and L. Pishkar, "Study of the prostate-specific antigen–aptamer stability in the PSA–aptamer-single wall carbon nanotube assembly by docking and molecular dynamics simulation", ***Mol Simul,*** 47, 951–959 (2021).
9. F. Morena, C. Argentati, I. Tortorella, C. Emiliani, S. Martino, "De novo ssRNA Aptamers against the SARS-CoV-2 Main Protease: In Silico Design and Molecular Dynamics Simulation", Int. J. Mol. Sci., , 22, 6874. (2021)
10. N. A. Ahmad, R. M. Zulkifli, H. Hussin, S. I. Amran, M. H. Nadri, S. I. A. Razak, *et al.*, "In silico evaluation of potential murine M49 DNA aptamer on ORF7a of SARS-COV-2: A similar target", ***J Res Pharm,*** 27(1), 232 (2023) .

11. H. S. Zarandi, M. Behbahani and H. Mohabatkar, "In silico selection of GP120 SSDNA aptamer to HIV-1", ***SLAS Discovery,*** 25(9), 1087-1093 (2020).
12. B. Ropii, M. Bethasari, I. Anshori, A. P. Koesoema, W. Shalannanda, A. Satriawan, C. Setianingsih, M. R. Akbar and R. Aditama, "The assessment of molecular dynamics results of three-dimensional RNA aptamer structure prediction", ***PloS One,*** 18(7), e0288684 (2023).
13. A. A. Buglak, A. B. Самохвалов, A. V. Zherdev and B. B. Dzantiev, "Methods and applications of in silico Aptamer design and modeling", ***Int J Mol Sci,*** 21(22), 8420 (2020).
14. A. M. Muhammad, A. Zari, N. H. Alsubhi, M. H. Al-Zahrani, R. Alghamdi and M. M. Labib, "Novel design of RNA aptamers as cancer inhibitors and diagnosis targeting the tyrosine kinase domain of the NT-3 growth factor receptor using a computational Sequence-Based approach", ***Molecules,*** 27(14), 4518 (2022).
15. J. Sarzyńska, M. Popenda, M. Antczak and M. Szachniuk, "RNA tertiary structure prediction using RNAComposer in CASP15", ***Proteins,*** 91(12), 1790–1799 (2023).
16. M. Popenda, M. Szachniuk, M. Antczak, K. J. Purzycka, P. Łukasiak, N. Bartol, J. Błażewicz and R. W. Adamiak, "Automated 3D structure composition for large RNAs", ***Nucleic Acids Res,*** 40(14), e112 (2012).
17. M. Remmert, A. Biegert, A. Hauser and J. Söding, "HHblits: lightning-fast iterative protein sequence searching by HMM-HMM alignment", ***Nat Methods,*** 9(2), 173–175 (2011).
18. W. R. Pearson and D. J. Lipman, "Improved tools for biological sequence comparison", ***Proc Natl Acad Sci USA,*** 85(8), 2444–2448(1988).
19. F. Sievers, A. Wilm, D. Dineen, T. J. Gibson, K. Karplus, W. Li, R. López, H. McWilliam, M. Remmert, J. Söding, J. Thompson and D. G. Higgins, "Fast, scalable generation of high-quality protein multiple sequence alignments using Clustal Omega", ***Mol Syst Biol,*** 7, 539 (2011).
20. M. A. Larkin, G. Blackshields, N. P. Brown, C. Ramu, P. McGettigan, H. McWilliam, F. Valentin, I. Wallace, A. Wilm, R. López, J. Thompson, T. J. Gibson and D. G. Higgins, "Clustal W and Clustal X version 2.0", ***Bioinformatics,*** 23(21), 2947–2948(2007).
21. M. A. Martí-Renom, A. C. Stuart, A. Fiser, R. Sánchez, F. S. Melo and A. Šali, "Comparative protein structure modeling of genes and genomes", ***Annu Rev Biophys Biomol Struct,*** 29, 291–325(2000).
22. H. M. Berman, "The Protein Data Bank", ***Nucleic Acids Res***, 28(1), 235–242(2000).
23. R. Ahirwar, S. Nahar, S. Aggarwal, S. Ramachandran, S. Maiti and P. Nahar, "In silico selection of an aptamer to estrogen receptor alpha using computational docking employing estrogen response elements as aptamer-alike molecules", ***Sci Rep,*** 6, 21285 (2016).
24. M. F. Adasme, K. L. Linnemann, S. N. Bolz, F. Kaiser, S. Salentin, V. J. Haupt and M. Schroeder, "PLIP 2021: expanding the scope of the protein–ligand interaction profiler to DNA and RNA", ***Nucleic Acids Res***, 49(W1), W530–W534(2021).
25. S. Jo, T.-H. Kim, V. Iyer, W. Im, "CHARMM-GUI: A web-based graphical user interface for CHARMM", ***J Comput Chem,*** 2008, 29(11), 1859–1865(2008).
26. B. R. Brooks, C. L. Brooks, A. D. MacKerell, L. Nilsson, R. J. Petrella, B. Roux, Y. Won, G. Archontis, C. Bartels, S. Boresch, A. Caflisch, L. S. D. Caves, Q. Cui and A. R. Dinner, "CHARMM: The biomolecular simulation program", ***J Comput Chem,*** 30(10), 1545–1614(2009) .
27. J. Lee, X. Cheng, J. Swails, M. S. Yeom, P. Eastman, J. A. Lemkul, S. Wei, J. Buckner, J. C. Jeong, Y. Qi, S.

Jo, V. S. Pande, D. A. Case, C. L. Brooks, A. D. MacKerell, J. B. Klauda and W. Im, "CHARMM-GUI Input Generator for NAMD, GROMACS, AMBER, OpenMM, and CHARMM/OpenMM simulations using the CHARMM36 Additive Force Field", ***J Chem Theory Comput,*** 12(1), 405–413(2015).

28. J. C. Phillips, R. Braun, W. Wang, J. C. Gumbart, E. Tajkhorshid, E. Villa, C. Chipot, R. D. Skeel, L. V. Kalé and K. Schulten, "Scalable molecular dynamics with NAMD", ***J Comput Chem,*** 26(16), 1781–1802(2005).
29. W. Humphrey, A. Dalke and K. Schulten, "VMD: Visual molecular dynamics", ***J Mol Graph,*** 14(1), 33–38(1996).
30. Y. Mo, "Probing the nature of hydrogen bonds in DNA base pairs", ***J Mol Model,*** 12(5), 665–672 (2006).
31. The PyMOL Molecular Graphics System, Version 3.0 Schrödinger, LLC. https://pymol.org/2/
32. R. Kothandan, P. Uthayasooriyan and S. Vairamani, "Search for RNA aptamers against non-structural protein of SARS-CoV-2: Design using molecular dynamics approach", ***Beni-Seuf Univ J Basic Appl Sci,*** 10(1), 64 (2021).
33. C. A. Almazar, M. V. Mendoza and W. L. Rivera, "In Silico Approaches for the Identification of Aptamer Binding Interactions to Leptospira spp. Cell Surface Proteins", ***Trop Med Infect Dis,*** 8(2), 125 (2023).
34. J. Jumper, R. Evans, A. Pritzel, T. Green, M. Figurnov, O. Ronneberger, K. Tunyasuvunakool, *et al.*, "Highly accurate protein structure prediction with AlphaFold", ***Natur,*** 596(7873), 583–589 (2021).
35. I. Tuszyńska, M. Magnus, K. Jonak, W. Dawson and J. Bujnicki, "NPDock: a web server for protein–nucleic acid docking", ***Nucleic Acids Res,*** 43(W1), W425–W430(2015).
36. A. Shraim, B. a. A. Majeed, M. A. Al-Binni and A. A. Hunaiti, "Therapeutic potential of Aptamer–Protein interactions", ***ACS Pharmacol Transl Sci,*** 5(12), 1211–1227(2022).
37. B. Lin, M. Zhu, W. Wang, W. Li, D. Xu, Y. Chen, Y. Lü, J. Guo and M. Li, "Structural basis for alpha fetoprotein-mediated inhibition of caspase-3 activity in hepatocellular carcinoma cells", ***Int J Cancer,*** 141(7), 1413–1421(2017).
38. M. Zhu, B. Lin, P. Zhou and M. Li, "Molecular Analysis of AFP and HSA Interactions with PTEN Protein", ***BioMed Res Int,*** 2015, 256916 (2015).
39. A. A. Terentiev, N. T. Moldogazieva, O. B. Левцова, D. M. Maximenko, D. A. Borozdenko and K. B. Шайтан, "Modeling Of Three Dimensional Structure Of Human Alpha-Fetoprotein Complexed With Diethylstilbestrol: Docking And Molecular Dynamics Simulation Study", ***J Bioinform Comput Biol,*** 10(2), 1241012 (2012).
40. J. Sharma, V. K. Bhardwaj, R. Singh, V. Rajendran, R. Purohit and S. Kumar, "An in-silico evaluation of different bioactive molecules of tea for their inhibition potency against non structural protein-15 of SARS-CoV-2", ***Food Chem,*** 346,128933 (2021).
41. S. Manandhar, R. Sankhe, K. Priya, G. Hari, H. K. B, C. H. Mehta, U. Y. Nayak and K. S. R. Pai, "Molecular dynamics and structure-based virtual screening and identification of natural compounds as Wnt signaling modulators: possible therapeutics for Alzheimer's disease", ***Mol Divers,*** 26(5), 2793-2811 (2022).
42. Z. K. Bagewadi, T. M. Y. Khan, B. Gangadharappa, A. Kamalapurkar, S. M. Shamsudeen and D. A. Yaraguppi, "Molecular dynamics and simulation analysis against superoxide dismutase (SOD) target of Micrococcus luteus with secondary metabolites from Bacillus licheniformis recognized by genome mining approach", ***Saudi J Biol Sci,*** 30(9), 103753(2023)
43. J. Kashyap and D. Datta, "Drug repurposing for SARS-CoV-2: a high-throughput molecular docking, molecular dynamics, machine learning,

and DFT study*", J Mater Sci,* 57(23), 10780–10802 (2022) .

44. S. A. Ejaz, M. Aziz, Z. Zafar, N. Akhtar and H. A. Ogaly, "Revisiting the inhibitory potential of protein kinase inhibitors against NEK7 protein via comprehensive computational investigations", ***Sci Rep,*** 13(1), 4304 (2023).
45. J. F. Fatriansyah, R. K. Rizqillah, M. Y. Yandi, F. Fadilah and M. Sahlan, "Molecular docking and dynamics studies on propolis sulabiroin-A as a potential inhibitor of SARS-CoV-2", ***J King Saud Univ Sci,*** 34(1), 101707(2022) .
46. S. Ahamad, D. Gupta and V. Kumar, "Targeting SARS-CoV-2 nucleocapsid oligomerization: Insights from molecular docking and molecular dynamics simulations", ***J Biomol Struct Dyn,*** 40(6), 2430–2443 (2020).
47. Y.-C. Lin, W.-Y. Chen, E. Hwu and W. Hu, "In-Silico selection of aptamer targeting SARS-COV-2 spike protein", ***Int J Mol Sci,*** 23(10), 5810 (2022).

Bull. Pharm. Sci., Assiut University, Vol. 47, Issue 2, 2024, pp. 989-1008.

نشرة العلوم الصيدلية
جامعة أسيوط

BULL. PHARM. SCI. Assiut Univ.

عنوان الاختيار والتحسين الحسابي لـ RNA APTAMER ضد ALPHA-FETOPROTEIN- دراسة حاسوبية

محمد محمد الكريز* – ديما جوجة

قسم هندسة التكنولوجيا الحيوية، كلية الهندسة التقنية، جامعة حلب، سوريا

سرطان الكبد هو السبب الرئيسي الرابع للوفاة المرتبطة بالسرطان، يسبب ما يقارب من ٧.٨ مليون حالة وفاة سنوياً. سرطان الخلايا الكبدية Hepatocellular carcinoma هو النوع الأكثر شيوعاً من سرطان الكبد.

في الدراسة الحالية، تم استخدام الأساليب الحسابية لتطوير أبتامير الحمض النووي الريبي (RNA) ضد بروتين AFP، وهو المؤشر الحيوي الأكثر استخداماً لسرطان الخلايا الكبدية (HCC). حيث تم استخدام تسلسلات RNA العشوائية كمصدر للدراسة، وتم إدخال عدة جولات من الطفرات إلى هذه التسلسلات لتعزيز تقارب الارتباط. تم تطبيق عمليات الالتحام الجزيئي والمحاكاة الديناميكية الجزيئية لدراسة التفاعلات بين الأبتامير المختار وبروتين AFP بالتفصيل. ونتيجة لذلك، أظهر الأبتامير المحدد تقارب ربط جيد للهدف AFP. حيث أظهرت دراسة كلا من RMSF، والروابط الهيدروجينية، وRMSD أن معقد بروتين الأبتامير لديه مرونة واستقرار خلال وقت المحاكاة.

وبناء على هذه التجارب، نقترح أن هذا الأبتامير يمكن أن يكون بمثابة مرشح جيد لتشخيص أو علاج سرطان الكبد.